

# Application of a noisy data classification technique to determine the occurrence of flashover in compartment fires

Eric W.M. Lee <sup>a,\*</sup>, Y.Y. Lee <sup>a</sup>, C.P. Lim <sup>b</sup>, C.Y. Tang <sup>c</sup>

<sup>a</sup> Department of Building and Construction, City University of Hong Kong, Tat Chee Avenue, Kowloon Tong, Kowloon, Hong Kong, China

<sup>b</sup> School of Electrical and Electronic Engineering, University of Science Malaysia, Penang, Malaysia

<sup>c</sup> Department of Industrial and Systems Engineering, Hong Kong Polytechnic University, Hung Hom, Kowloon, Hong Kong, China

Received 17 May 2005

## Abstract

This paper presents a hybrid Artificial Neural Network (ANN) model that is developed for noisy data classification. The model, named GRNNFA, is a fusion of the Fuzzy Adaptive Resonance Theory (FA) model and the General Regression Neural Network (GRNN) model. The GRNNFA model not only retains the important features of the parent models, which include stable learning, fast training, and an incremental growth network structure, but also facilitates the removal of noise that is embedded in training samples. The robustness of the GRNNFA model is demonstrated by the Noisy Two Intertwined Spirals problem and other benchmarking problems. The model is then applied to Fisher's Iris Data, which is a real-world classification problem. The results show that the percentage of correct predictions is statistically higher than in variant models of the adaptive resonance theory. The GRNNFA is further employed in a new application area of soft computing—fire dynamics, which is highly non-linear in nature. Flashover is the most dangerous scenario in the development of a compartment fire, during which, any unburned combustible material, including the unburned soot particles inside the compartment, is ignited spontaneously and all combustible material is then simultaneously involved in the burning process. The GRNNFA model is applied to predict the occurrence of the flashover in compartment fires based on the fire size and the geometry of the fire compartment. The performance of the GRNNFA is compared with other published results, and it is shown to be statistically superior to other ANN models.

© 2005 Elsevier Ltd. All rights reserved.

*Keywords:* Compartment fire; Flashover; Fuzzy ART; General regression neural network; GRNNFA

## 1. Introduction

Many buildings and constructions are extensively equipped with various fire extinguishing systems (e.g. fire detection systems, sprinkler systems, and fire hydrant systems) to minimize the extent of destruction and the number of fatalities in fire cases. Nevertheless, fire, which consists of many associated and dynamically interacting physical and chemical processes that are non-linear in nature, is still considered to be a major threat due to many circumstances. If there is no proper means of control, then fires can be potentially lethal. Over the past few decades, scientists and engineers have invested considerable effort in investigating the dynamic behavior of fires. Experiments and numerical modeling techniques have been developed to improve fire extinguishing systems and to

reduce fire risks. However, because fire experiments are rather destructive and expensive, they are rarely carried out, and even when they are, most of them are restricted to simple geometrical structures. As a result, various numerical approaches, such as zone and field models, have been developed to provide a better understanding of fires. In particular, the surge in the application of fire field models that are based on the application of computational fluid dynamic (CFD) techniques [1–10] to fire problems clearly shows the desire to better understand and predict fire scenarios. However, for fire safety engineering designs, it is well recognized that these fire field models usually require extensive computational resources (especially, lengthy computational times over a large number of grids) to provide useful information, such as transient hot smoke layer height and temperature distribution. These models are therefore often limited to application in the fire safety engineering design of projects of considerably large-scale. The facilitation of the efficient and economical application of fire models to medium- and small-scale engineering projects through the shortening of

\* Corresponding author. Tel.: +852 2194 2307; fax: +852 2784 4655.

E-mail address: [ericlee@cityu.edu.hk](mailto:ericlee@cityu.edu.hk) (E.W.M. Lee).

computer simulation time remains an unresolved but urgent and important task for the fire research community.

Because of its superior ability to capture non-linear system behavior and its extremely fast computational speed in making predictions, the artificial neural network (ANN) model is an alternative that can be applied to simulate the behavior of fires by learning the history of the fire system. Currently, ANN techniques have only been applied to fire detection systems [11–15]. Such studies have confirmed the applicability of ANN techniques, which have shown superior performance compared to other traditional models, but the actual application of ANN techniques to determine the consequences of fire is still very limited. Lee et al. [16] applied the Feedforward Multi-layered Perceptron (MLP) model [17] to the determination of sprinkler actuation. The prediction results were found to be comparable to the zone fire models. The Fuzzy ARTMAP (FAM) model that was developed by Carpenter et al. [18] was employed by Lee et al. [19] to determine the occurrence of flashover. The highest rate of correct prediction was determined to be 97.6%. Lee et al. also developed a probabilistic inference engine (PEMap) [20] that is based on the theory of maximum information entropy to deal with the uncertainties that are embedded in fire data. This engine is also applied to determine the occurrence of flashover. The results show that the performance of the PEMap is competitive with that of FAM, but it has a comparatively simple network structure and working mechanism. These pioneer studies have confirmed the applicability of ANN techniques in terms of determining the consequences of fire.

The quality and quantity of available training samples are critical to the success of ANN predictions. Due to the dynamic behavior of fire and the high costs of full-scale fire experiments, the actual data that are collected from existing fire experiments are usually limited and noisy in nature. The GRNNFA model [21] was specifically designed to remove the noise that is embedded in training samples, and to change the network complexity incrementally according to the distribution of the training dataset. The GRNNFA model has been intensively examined and its superior performance in noisy data regression has been demonstrated [21]. The GRNNFA model has also been successfully applied to predict the height of the thermal interface in compartment fires [22]. In this paper, the GRNNFA model is applied to determine the most important stage in the development of a compartment fire—flashover.

Flashover is an intermediate stage in the development of a compartment fire. A typical compartment fire growth characteristic curve is shown in Fig. 1. At the initial stage, which is called the growth phase, the fire continues to grow in the presence of sufficient oxygen and fuel. The fire plume is then established and transfers the heat energy to the upper part of the compartment. When the hot gas reaches the ceiling, it spreads and reaches the boundary walls and then starts to accumulate in the upper part of the compartment and descend downwards. The layer of hot gases and the fire plume emit radiant heat, which raises the temperature of the surrounding combustible material. When the intensity of this radiation is sufficiently high, the temperature of the surrounding combustible material

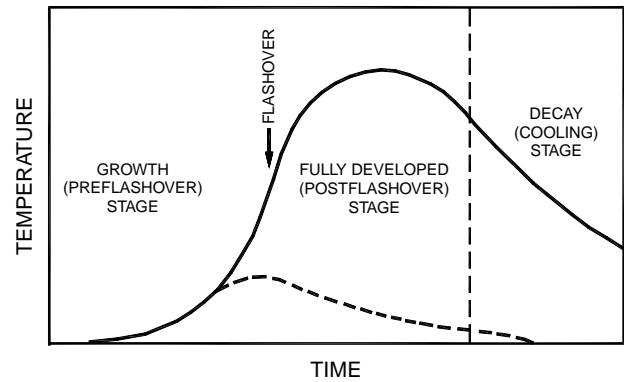


Fig. 1. Development of a compartment fire. Flashover is the intermediate stage between the pre-flashover and post-flashover stages. At the flashover stage, any unburned combustible material inside the fire compartment is ignited by the radiant heat that is released from the hot gases created by the fire.

is raised to their spontaneous ignition temperatures, and all of the combustible material is ignited at the same time, creating a most lethal fire scenario known as ‘flashover’. Different physical definitions of flashover are summarized in [23,24]. However, the most widely adopted criteria for the occurrence of the flashover stage is a scenario in which the hot gas temperature at 10 mm below the ceiling reaches 600 °C [25]. These criteria are adopted also in this study. After the flashover stage (the post-flashover stage), all of the combustible material inside the compartment is involved in the burning process. The total heat release rate becomes steady, and reaches the highest level. The fire continues to consume the combustible material as well as the oxygen inside the compartment. The heat release rate of the fire will be reduced when either the fuel or the oxygen inside the compartment is exhausted, which is the start of the decay stage. When all of the combustible material has been consumed or the oxygen content is lower than the threshold level, the fire will extinguish itself.

The structure of the rest of this paper is as follows. Section 2 introduces the formulation of the GRNNFA model. Section 3 describes the benchmarking results of the noisy data classification problems. Section 4 details the methodology for the application of the GRNNFA to predict the occurrence of the flashover, and the predicted results are discussed. Section 5 concludes the paper.

## 2. Formulation of the GRNNFA model

The GRNNFA model is a hybrid model that combines the GRNN and FA models. It retains the advantages of stable learning and fast training, and also facilitates noise removal. Here, the requirements for the predefinition of the network structure are absent, and the network can automatically and incrementally grow according to the sequence of the presentation of the training samples. One of the litmus tests of the GRNNFA model is its ability to be sufficiently trained with a limited amount of sample data to provide qualitative and quantitative predictions. Conventional ANN models usually require large amounts of sample data for training to effectively

generate reliable predictions, which is not possible in the area of fire, because the amount of data that exists for training purposes is limited and finite, and the samples are noisy in nature. This new GRNNFA model has thus been developed to address these problems.

The GRNNFA model comprises two modules: the FA, employed for network training, and the GRNN, employed for prediction. The basic approach to combining the GRNN and FA models is first to group all of the training samples into fewer numbers of prototypes using the FA. Upon completion of the grouping, the prototypes of the FA are converted to kernels in the GRNN module, which can then be used for prediction. The architecture of the GRNNFA model is shown in Fig. 2. A prototype created by the FA model is represented by the two vertices of the hyper-rectangle and is stored in field  $F_2$  of the module. As the format of the prototype is totally different from that of the kernel which is stored in the GRNN module, a conversion scheme is deployed to obtain the three parameters of each Gaussian kernel (the center, output, and width) from the corresponding hyper-rectangle.

During the training phase, the FA is employed to group the training samples into a set of hyper-rectangular prototypes. (Refer Fig. 2) The vigilance parameter  $\rho$  of the FA module, as described in Ref. [26], controls the maximum size of the prototypes to be created, which will adjust the resolution detail of the behavior that is to be stored. Upon the completion of the training phase, a compression scheme is employed to convert the hyper-rectangles of the FA model to the Gaussian kernels of the GRNN module. Eqs. (1) and (2) are the basic formulations of the GRNN module and of the GRNNFA model with multiple hyper-spherical kernels. Please refer to [27,28] for more details

on the GRNN model.

$$\hat{y}(\mathbf{x}) = \frac{\sum_{j=1}^n \frac{A_j}{\sigma_j^m} \exp \left[ -\frac{1}{2} \sum_{p=1}^m \left( \frac{x_p - \alpha_{jp}}{\sigma_j} \right)^2 \right]}{\sum_{j=1}^n \frac{B_j}{\sigma_j^m} \exp \left[ -\frac{1}{2} \sum_{p=1}^m \left( \frac{x_p - \alpha_{jp}}{\sigma_j} \right)^2 \right]} \tag{1}$$

$$\begin{cases} A_j^{(t+1)} = A_j^{(t)} + b_j \\ B_j^{(t+1)} = B_j^{(t)} + 1 \end{cases} \tag{2}$$

where

- $\hat{y}$  is the predicted output,  $\mathbf{x}$  is the input vector,
- $x_p$  is the  $p$ th of  $\mathbf{x}$ ,  $n$  is the total number of kernels,
- $m$  is the size of the input vector,  $\alpha_{jp}$  is the  $p$ th component of the kernel  $j$  center, and
- $\sigma_j$  is the spread of the kernel  $j$ ,  $b_j$  is the output clustered to kernel  $j$ .

The compression scheme for obtaining the three important parameters of the Gaussian kernels (the center, label, and width) of the GRNN module from the information in the prototypes of the FA module (the vertices of the hyper-rectangles) is described below.

### 2.1. Kernel center estimation

The FA is applied to establish prototypes in the input domain according to the distribution of the inputs of the samples. A prototype that is created by the FA is proposed for conversion to the center of the corresponding kernel by the method that is employed by Lim and Harrison [29,30].

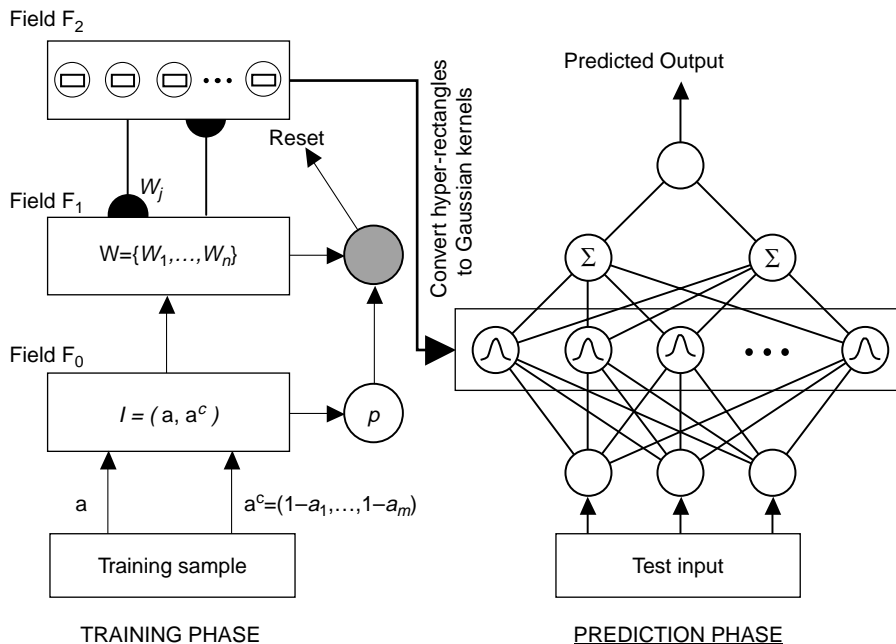


Fig. 2. Architecture of the GRNNFA model. It consists of the FA module (left of the figure) and the GRNN module (right of the figure). A compression scheme was developed to convert the information of the prototypes created by the FA module to the Gaussian kernels of the GRNN module.

The kernel center  $\mu_j$  of cluster  $J$  is determined by Eq. (3), where  $\mathbf{a}_{ji}(i=1,2,\dots,N_j)$  is the  $i$ th sample that is grouped into cluster  $J$  and  $N_j$  is the total number of samples inside this cluster.

$$\mu_j = \frac{\sum_{i=1}^{N_j} \mathbf{a}_{ji}}{N_j} \quad (3)$$

### 2.2. Kernel label estimation

A statistical regression model can be developed by taking the expected value over  $n$  number of kernels, as shown in Eq. (4), where  $\hat{y}$ ,  $\xi_j$ , and  $P(\theta_j|\mathbf{x})$  are, respectively, the predicted output, the label of the kernel  $\theta_j$ , and the probability of kernel  $\theta_j$  given the input vector  $\mathbf{x}$ .

$$\hat{y} = E(y|\mathbf{x}) = \sum_{j=1}^n \xi_j P(\theta_j|\mathbf{x}) \quad (4)$$

By applying Bayesian theory to Eq. (4) the regression model that is shown in Eq. (5) can be obtained.

$$\hat{y} = \frac{\sum_{j=1}^n \frac{N_j \xi_j}{\sigma_j^m} \exp \left[ -\frac{1}{2} \sum_{p=1}^m \left( \frac{x_p - \alpha_{jp}}{\sigma_j} \right)^2 \right]}{\sum_{j=1}^n \frac{N_j}{\sigma_j^m} \exp \left[ -\frac{1}{2} \sum_{p=1}^m \left( \frac{x_p - \alpha_{jp}}{\sigma_j} \right)^2 \right]} \quad (5)$$

The format of Eq. (5) is very similar to that of Eq. (1). It can be observed that  $N_j$  in the denominator of Eq. (5) (the total number of samples of kernel  $\theta_j$ ) is exactly equal to the value of  $B_j$  in Eq. (2) by definition. To obtain a statistically justified prediction model, it is proposed to equate  $N_j \xi_j$  in Eq. (5) to  $A_j$  in Eq. (1), i.e.

$$\xi_j = \frac{A_j}{N_j} \quad (6)$$

According to Eq. (6), the centroid of the output vectors of the clustered input samples should be taken as the label of kernel  $\theta_j$ .

This compression scheme also facilitates the removal of symmetrically distributed noise that is embedded in the training samples. Let  $\Psi_j \in \mathbb{R}^m$  be a subspace of the input domain that covers the prototype  $j$  that is created by the FA in which the samples  $\{\mathbf{a}_{j1}, \mathbf{a}_{j2}, \dots, \mathbf{a}_{jN_j}\} \in \Psi_j$  are clustered and let  $b=f(\mathbf{a})$ , i.e. be the underlying scalar function and  $\tilde{b}$  the noise-corrupted output that correspond to the input  $\mathbf{a}$ . The corrupted output can be separated into clean and noisy components, as shown in Eq. (7), where  $\varepsilon$  is the symmetrically distributed noise with zero mean:

$$\tilde{b}_{jk} = f(\mathbf{a}_{jk}) + \varepsilon(\mathbf{a}_{jk}) \quad \forall \mathbf{a}_{jk} \in \Psi_j \quad (7)$$

By integrating Eq. (7) over the subspace  $\Psi_j$ , the noise content is removed, which gives Eq. (8).

$$\int_{\Psi_j} \tilde{b} d\Psi = \int_{\Psi_j} b d\Psi \quad (8)$$

Eq. (8) can be discretized and formulated into Eq. (9).

$$\sum_{k=1}^{N_j} \tilde{b}_{jk} = \sum_{k=1}^{N_j} b_{jk} \quad (9)$$

The centroids of the clean outputs and the corrupted outputs can be obtained by dividing Eq. (9) by  $N_j$ :

$$\xi_j = \frac{\sum_{k=1}^{N_j} b_{jk}}{N_j} = \frac{\sum_{k=1}^{N_j} \tilde{b}_{jk}}{N_j} \quad (10)$$

Eq. (10) implies that the centroid of the clean outputs over  $\Psi_j$  can be obtained by projecting the centroid of the noise-corrupted outputs in  $\Psi_j$  to the output domain. This determination of clean information from the available noise-corrupted information demonstrates the noise removal.

### 2.3. Kernel width estimation

Multiple hyper-spherical kernels that are similar to those in Ref. [28] are adopted in the development of the GRNNFA model. Every kernel has its own radius of spread, and hence the total number of kernel widths to be determined equals the total number of kernels. Traditional approaches that are driven by the error gradient become inefficient in determining large sets of parameters. Here, the K-nearest-neighbors (kNN) approach is proposed to evaluate the widths of the multiple hyper-spherical kernels by the determination of a single parameter. Each kernel width is determined according to Eq. (11), which is similar to the scheme that is proposed by Lim and Harrison [29,30], except that the number of the nearest neighbors varies.

$$\sigma_j = \frac{1}{2\kappa} \sum_{k=1}^{\kappa} \|\mathbf{x}_j - \mathbf{x}_k\| \quad j \neq k \quad 1 \leq \kappa \in \mathbf{I}^+ \leq N-1 \quad (11)$$

The width of kernel  $j$  is set to be half of the average distance over  $\kappa$  numbers of the nearest neighbors to kernel  $j$ . By using an appropriate value for  $\kappa$  and the vigilance parameter of the FA model, a network structure with close to minimum validation error can be achieved. The concept of this approach is similar to the smoothing parameter of the original GRNN model. The probability density surface that is created by the Parzen Density Estimator [31] can be smoothed by increasing the value of  $\kappa$ . By suitably adjusting the value of  $\kappa$ , the close optimum set of the kernel widths can be obtained.

After being converted to the kernels of the GRNN module by the proposed compression scheme, the prototypes that are stored in field  $F_2$  of the FA module can then be used directly as the original GRNN model for network prediction. In the prediction phase, a test sample is fed to all of the kernels when it is presented to the GRNN module. The outputs from the kernels in response to the input vector are weighted and fed to the nominator and denominator nodes of the summation layer. The final prediction is obtained by dividing the output of the numerator node by that of the denominator node.

### 3. Benchmarking

#### 3.1. Noisy two intertwined spirals

The original Two Intertwined Spirals synthetic benchmark problem was designed by Land and Witbrock [32] to test the performance of classifiers on binary classes, which is regarded as a hard classification problem [33]. It was also employed by Carpenter et al. to evaluate the performance of the FAM [18]. In this benchmarking problem, two spirals, each of which has three complete turns, are created inside a unit square  $([0,1]^2 \in \mathbb{R}^2)$ . The task of the classifier is to discriminate the unit square domain from either of the two spiral regions. There are 194 clean samples (97 samples per spiral), which are created with the equations as shown in Ref. [18], where  $\{a_1^{(t)}, a_2^{(t)}\} \in \mathcal{X}$  is the location of the sample  $t$  at the input domain and the corresponding output is  $b^{(t)} = \begin{pmatrix} 1 \\ 0 \end{pmatrix}$ , the value of which is either 1 or 0. The distribution of the 194 clean samples over the  $[0,1]^2$  space is shown in Fig. 3.

$$\begin{cases} a_1^{(2n-1)} = 1 - a_1^{(2n)} = r_n \sin(\alpha_n) + 0.5 \\ a_2^{(2n-1)} = 1 - a_2^{(2n)} = r_n \sin(\alpha_n) + 0.5 \\ b^{(2n-1)} = 1 \\ b^{(2n)} = 0 \end{cases} \quad \text{where } n = 1, 2, \dots, 97.$$

$$\begin{cases} r_n = 0.4 \left( \frac{105 - n}{104} \right) \\ \alpha_n = \frac{\pi(n-1)}{16} \end{cases}$$

Williamson modified the data generation of the Two Intertwined Spirals to test the performance of the Gaussian ARTMAP [34] in a noisy environment by introducing Gaussian noise  $N(0,0.025)$  into the positions of the clean samples. Three test cases A, B, and C with 100, 1000, and 10,000 noise-corrupted samples, respectively, were used to test the performance of the GRNNFA model under different numbers of training samples.

After several trials, the vigilance parameter of the GRNNFA model was set to 0.95 and the value of  $\kappa$  was found to be 2. A total of 20 trials were performed for each of the cases with different random seeds. As the noise-corrupted samples in this study may not be exactly the same as those in Ref. [34], bootstrapping [35,36] techniques were applied. In each test case, the results of the 20 trials were used to obtain the bootstrap mean with 2000 re-samplings. The bootstrap mean of each pixel of the reconstructed images was taken as the prediction result. The images were discretized by setting the demarcation at the value of 0.5 to either 0 or 1. The images that were reconstructed by the GRNNFA and the Gaussian ARTMAP [34] are depicted in Fig. 4, which clearly shows that, referring to the distribution of the clean samples as shown

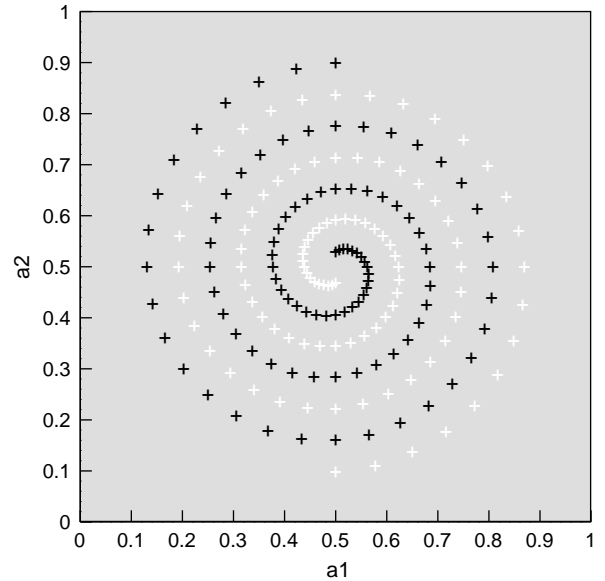


Fig. 3. Distribution of 194 clean samples. For easy visualization, white and black crosses that are shown in the figure indicate the values of 0 and 1, respectively. The training samples for the Noisy Two Intertwined Spirals problem are prepared by introducing Gaussian noise (0,0.025) to the horizontal and vertical positions of each clean sample.

in Fig. 3, the quality of the spirals that were reconstructed by the GRNNFA is better than those reconstructed by the Gaussian ARTMAP [34].

#### 3.2. Fisher's Iris Data

Fisher [37] introduced a benchmark dataset that contains the sepal and petal measurements of different types of iris flowers. The dataset can be downloaded from the website of the UCI repository ([www.ics.uci.edu/~mllearn/MLRepository.html](http://www.ics.uci.edu/~mllearn/MLRepository.html)). There are 150 training samples, each of which consists of four inputs and one output. The inputs are the measured lengths and widths of the petals and the sepals, and the output is the type of iris flower, such as Setosa, Versicolor, and Virginica. The three types of iris flowers are shown in Fig. 5. The distributions of the samples with respect to the dimensions of the sepals and petals are shown in Fig. 6 for easy visualization. It reveals that the classes of Versicolor and Virginica overlap in both figures, whereas the class of Setosa is clearly separated from the other two classes.

This classification benchmarking problem was used to evaluate the performance of Falcon-ART [38] and Falcon-ModifiedART (Falcon-MART) [39]. Falcon-MART was developed to tackle the poor performance of Falcon-ART when the classes of input data are similar and with poor resistance to noise samples [39].

Falcon-ART is a neuro-fuzzy system that adaptively increases the number of membership functions in the input and output domains using Fuzzy ART according to the complexities of the data distribution. It basically consists of five layers, namely the input crisp layer, the input linguistic layer, the rule layer, the output linguistic layer, and the output

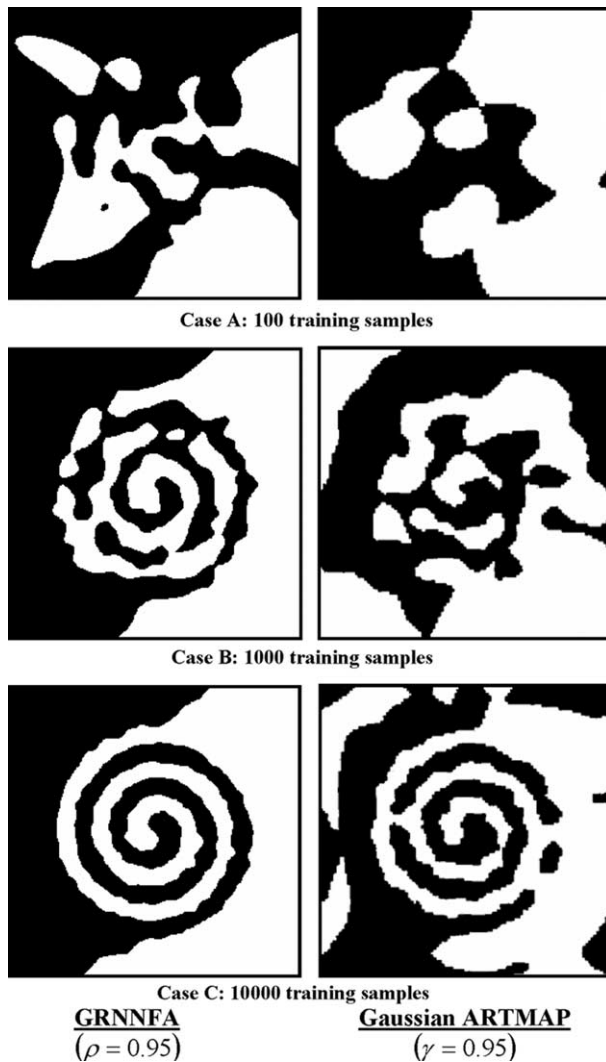


Fig. 4. The spirals reconstructed by the GRNNFA and the Gaussian ARTMAP. The quality of the image reconstructed by the GRNNFA is clearly better than that by the Gaussian ARTMAP (Williamson, 1996).

crisp layer. FA is applied to autonomously increase the partition of the input and output domains, or the number of membership functions, and the input and output linguistic layers are connected by the rule layer. Fisher's Iris Data was applied to Falcon-ART by Ref. [39] to illustrate the shortcomings of the model, which was subsequently improved as Falcon-MART [39]. The major improvements are the magnification of the difference in output values of the

membership functions of the same attribute to distinguish the class of input sample and apply the slow learning of Fuzzy ART to accommodate the network operation in a noisy environment.

The Fisher's Iris Data was employed to evaluate the performance of Falcon-ART and Falcon-MART in a noisy environment. The dataset contains 150 samples. The number of samples for network training and testing strictly followed [39], and were set to be 35 and 65%, respectively. The same procedures were followed in this study to evaluate the performance of the GRNNFA model. After several trials, the best value of the vigilance parameter was found to be 0.95 and the corresponding best value of  $\kappa$  was determined to be three. Twenty experiments were conducted with a random selection of data for network training and testing. The prediction results were concluded by estimating the mean and standard deviation of the percentage of correct predictions for comparison with the predictions of Falcon-ART and Falcon-MART, as shown in Table 1. It can be observed that the GRNNFA model has the highest percentage of correct predictions, and that the corresponding standard deviation of the GRNNFA model is lower than that of both Falcon-ART and Falcon-MART. It can be preliminarily concluded that GRNNFA outperforms the Falcon models in this benchmarking problem with high stability, which indicates that the GRNNFA model is less sensitive to noisy training samples (the samples in the overlapped region). As the training and testing samples were selected at random from the original dataset, the bootstrap technique was applied to obtain a more representative result. Table 2 shows the bootstrapped results with different numbers of re-samplings. The changes in confidence limits and the mean of the bootstrapping are less than 0.0003% with 1600 re-samplings and above. The results that are obtained from the 1600 re-samplings are selected. It can also be observed that the lower limit of the 95% confidence interval (95.7071%) is higher than the mean values of both Falcon-ART and Falcon-MART. It can be concluded that the performance of the GRNNFA model is statistically superior to both Falcon-ART and Falcon-MART in this noisy classification benchmarking problem. Here, the standard deviations of Falcon-ART (7.54%) and Falcon-MART (4.64%), which were obtained from only three trials [39], are considered unjustified. The standard deviation of the percentage of correct predictions of the GRNNFA model (0.88%) is indicated in Table 1 for the sake of complete and like for like comparison. To avoid

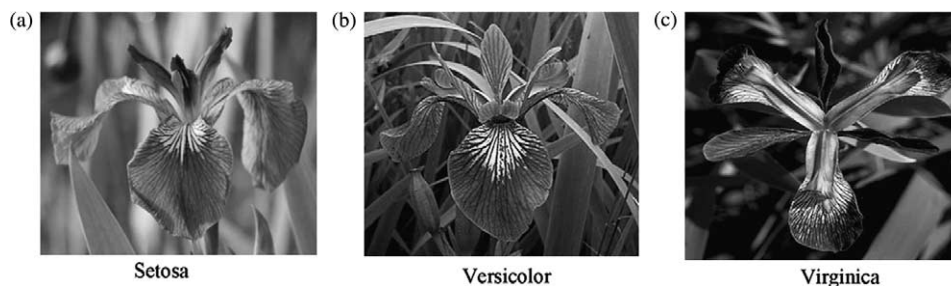


Fig. 5. Iris Setosa, Versicolor and Virginica flowers. The photos are from <http://www.evim.ethz.ch/uebungen/praxis/u3/irisbilder.htm>.

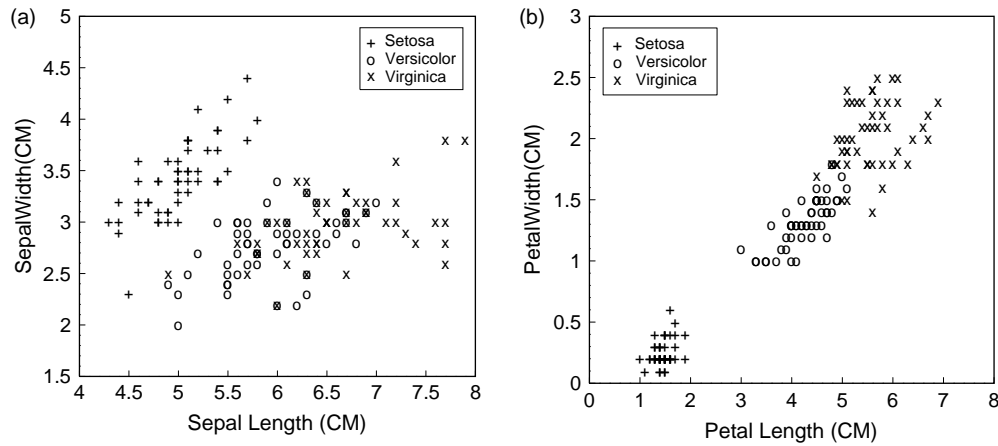


Fig. 6. Distribution of iris data with respect to the sepal and petal dimensions.

misclassification, a confusion matrix approach is adopted. The columns and rows indicate the target classes and predicted classes, and the number of samples that are misclassified is shown in the off-diagonal elements. In an ideal situation of 100% correct prediction in all classes, the value of the off-diagonal elements should be zero to reflect zero misclassification cases. Each element of the confusion matrix that is represented in the form of the mean and limits of the 95% confidence interval is obtained at by bootstrapping with 1600 re-samplings from the 20 trials. The results are shown in Table 3.

The reason that no sample has been misclassified as Setosa, according to Fig. 6 is because the Setosa samples are locationally remote from the other two classes. As there is no overlapping between the Setosa and the other two classes, the decision boundary can be identified clearly, and thus the rate of misclassification is zero. However, misclassifications were found in the classes of the Versicolor and Virginica because the samples for these two classes are very similar (overlap) and are difficult to distinguish [39]. Nevertheless, the overall performance of GRNNFA is considered superior to both the Falcon-ART and Falcon-MART models.

#### 4. Predicting the occurrence of flashover in compartment fire

As it is expensive to obtain real fire data from full-scale model experiments, computational fire simulations created by computer software are usually employed to generate data sets for the training of the GRNNFA model. The fire compartment,

for simplicity, is assumed to be rectangular in shape with an open door as illustrated in Fig. 7.

The interaction between fire and the environmental parameters has been proposed by McCaffrey et al. [40]. In his model, the temperature of the upper hot gas layer is a function of the room geometry, including the dimensions of the opening, the properties of the gas, the wall conduction characteristics, and the heat release rate. The criteria for flashover as defined by Hägglund et al. [24] were adopted in this study, and were inputted into the computer package FASTLite [41] to estimate the occurrence of flashover. The engine for this computer package is FAST [42]. This benchmarking test is a four-input and one-output classification problem. In the computer simulation, the following parameters

Table 2  
Bootstrap means and confidence limits of MSE for the Fisher’s Iris Data problem

No. of re-sampling	Lower limit of the 95% confidence interval	Upper limit of the 95% confidence interval	Mean
200	95.6566	96.5152	96.0987
400	95.7071	96.5152	96.1184
800	95.7576	96.5152	96.1196
1600	95.7071	96.5152	96.1119
3200	95.7071	96.5152	96.1121
6400	95.7071	96.5152	96.1106

Table 1  
Prediction result of Fisher’s Iris Data by the GRNNFA compared with the results predicted by the Falcon-ART and Falcon-MART adopted from Quek and Tang (2001)

Model	Mean of percentage of correct prediction (%)	Standard deviation of percentage of correct prediction (%)
Falcon-ART	75.76	7.54
Falcon-MART	94.95	4.64
GRNNFA	96.11	0.88

Table 3  
Confusion matrix of the GRNNFA prediction on Fisher’s Iris Data

Target classes	Predicted classes		
	Setosa	Versicolor	Virginica
Setosa	32.74% (31.35, 34.25%)	0.00% (0.00, 0.00%)	0.00% (0.00, 0.00%)
Versicolor	0.05% (0.00, 0.15%)	31.31% (30.30, 32.35%)	2.00% (1.55, 2.50%)
Virginica	0.00 (0.00, 0.00%)	1.79 (1.35, 2.25%)	31.10 (29.45, 32.60%)

Bracketed figures are the limits of the 95% confidence interval.

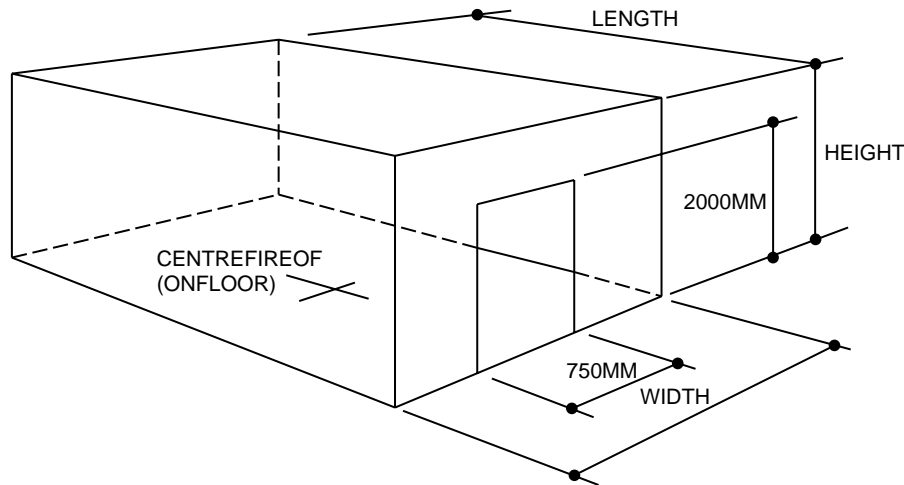


Fig. 7. Fire compartment for modeling the occurrence of flashover.

were randomly generated for the network training, and served as the inputs of the GRNNFA model:

- room length (varies randomly from 2 to 10 m),
- room width (varies randomly from 2 to 10 m),
- room height (varies randomly from 2 to 10 m), and
- maximum heat release rate (varies randomly from 10 to 6000 kW).

Fast growth t-square ( $t^2$ ) fire [43] was also assumed throughout the simulation. The growth of the  $t^2$ -fire is described by the expression  $\dot{Q} = \alpha(t - t_i)^2$ , where  $\dot{Q}$  is the heat release rate (kW),  $\alpha$  is the growth constant ( $0.0469 \text{ kW s}^{-2}$ ),  $t_i$  is the initial time (s), and  $t$  is the time (s).

The ceiling and walls in the fire simulation were assumed to be made of 16-mm gypsum, and the floor was assumed to be 12.7-mm plywood. For the different combinations of room

dimensions and maximum heat release rates, the occurrences of flashover as determined by FASTlite [41] were recorded for network training and testing. Three hundred and seventy-five samples were generated, of which 190 were flashover samples and 185 were non-flashover samples. Fig. 8 shows the distribution of the samples. It can be seen that the classes of flashover and non-flashover overlap, which creates a difficulty in drawing the decision boundary between the two classes.

Two hundred and fifty samples were randomly drawn from the original 375 samples for network training. The other samples (125 samples) were reserved to test the performance of the trained network. The prediction errors of the GRNNFA model were also compared with those of FAM and PEMap as shown in Lee et al. [20].

The GRNNFA model was applied to predict the occurrence of flashover under the given fire scenario parameters (length, width, and height of the compartment and the maximum heat release rate). After several trials, the vigilance parameter was set to be 0.86. The following confusion matrix shows the best result has been predicted by the GRNNFA model.

It can be observed that the confusion matrix as shown in Table 4 is symmetric and diagonally dominant, indicating that the GRNNFA predicted the occurrence of flashover with minimum bias to either class with a misclassification rate of less than 4% (1.6% + 1.6%). The prediction result is excellent from an engineering point of view. The percentage of correct predictions of non-flashovers is less than the correct percentage of prediction of flashovers in this binary decision problem,

Table 4  
Confusion matrix of the GRNNFA prediction on the occurrence of flashover in a compartment fire

No. of cases	Cases predicted by the GRNNFA to be non-flashover	Cases predicted by the GRNNFA to be flashover
Cases of non-flashover in test samples	58 (46.4%)	2 (1.6%)
Cases of flashover in test samples	2 (1.6%)	63 (50.4%)

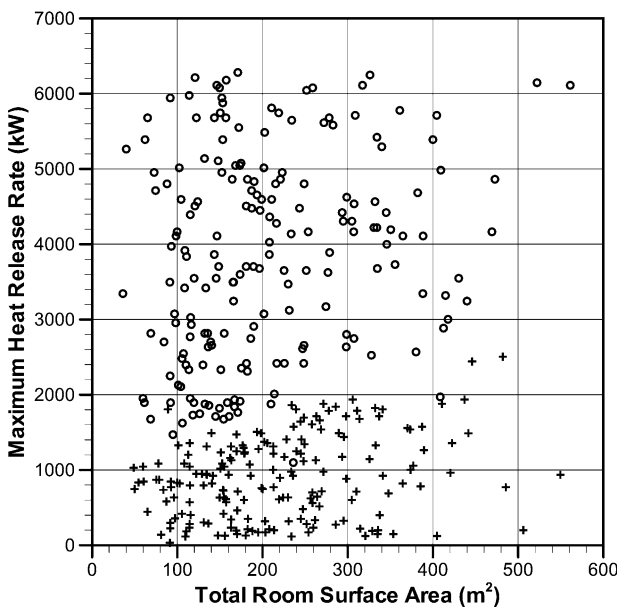


Fig. 8. Data distribution for network training and testing (+ : non-flashover, o: flashover).

Table 5

Bootstrapping results of percentage of correct prediction by the GRNNFA on the occurrence of flashover in a compartment fire with different re-sampling numbers

No. of re-sampling	Lower limit of 95% confidence interval	Mean	Upper limit of 95% confidence interval
200	91.92	92.6101	93.34
400	91.82	92.6158	93.36
800	91.78	92.5561	93.28
1600	91.78	92.6023	93.36
3200	91.86	92.6017	93.34
6400	91.86	92.6113	93.36
12800	91.86	92.5997	93.36

because the number of non-flashovers samples (185 samples) is less than that of the flashover samples (190 samples). The knowledge that was contributed about non-flashovers was hence less than that of flashovers, which led to the lower percentage of correct predictions in the non-flashover cases.

As a randomization process was involved in the procedures for the performance evaluation (the random extraction of samples for network training and testing), the bootstrapping technique was applied to statistically reveal the actual performance of the GRNNFA model. Forty experiments with different random data extraction for the training and test datasets were carried out. Bootstrapping procedures with different numbers of re-samples were applied to the 40 experimental results. The results are shown in Table 5.

Owing to the small variation (less than 0.02%) in the means and confidence limits of the Root Mean Squared Error (RMSE), the results that were obtained from 6400 re-samplings were taken. Table 6 shows that the percentage of correct predictions of both FAM and PEMap were lower than the lower limit of the 95% confidence interval of the GRNNFA model, and that is clearly demonstrates the superior performance of GRNNFA compared with the other two models in the determination of the occurrence of flashover.

## 5. Conclusions

The GRNNFA model that was developed for working in noisy environment has been introduced. It has been critically examined (Lee et al., 2004). The result of the Noisy Two Intertwined Spirals problem has demonstrated the noise removal feature of the GRNNFA model, which has also been applied to Fisher's Iris Data problem. The result shows that the performance of the GRNNFA is superior to that of the Falcon

Table 6

Percentages of correct predictions by FAM, PEMap, and GRNNFA on the occurrence of flashover in a compartment fire

Model	Percentage of correct prediction (%)
FAM	91.2
PEMap	91.8
GRNNFA	92.60 (91.86, 93.36%)

Bracketed figures are the lower and upper limits of the 95% confidence interval of the bootstrapped results.

ART family of models, which were developed for working in a noisy environment. The GRNNFA has been applied to determine the occurrence of flashover in compartment fires. Noise that was created by computer simulation was introduced into the training samples, and the result shows that the performance of the GRNNFA model is statistically superior to that of the Fuzzy ARTMAP and PEMap models in this application.

## References

- [1] Chow WK. A comparison of the use of fire zone and field models for simulating atrium smoke-filling processes. *Fire Saf J* 1995;25(4):337–53.
- [2] Chow WK. Use of computational fluid dynamics for simulating enclosure fires. *J Fire Sci* 1995;13(4):300–34.
- [3] Chow WK. On smoke control for tunnels by longitudinal ventilation. *Tunneling Underground Space Technol* 1998;13(3):271–5.
- [4] Chow WK, Cui E. CFD simulations on balcony spill plume. *J Fire Sci* 1998;16(6):468–85.
- [5] Beard AN. Fire models and design. *Fire Saf J* 1997;28:117–38.
- [6] Yeoh GH, Yuen RKK, Lo SM, Chen DH. On numerical comparison of enclosure fire in a multi-compartment building. *Fire Saf J* 2003;38:85–94.
- [7] Yeoh GH, Yuen RKK, Chen DH, Kwok WK. Combustion and heat transfer in compartment fires. *Numer Heat Transfer Part A—Appl* 2002; 42(1–2):153–72.
- [8] Yeoh GH, Yuen RKK, Cheung SCP, Kwok WK. On modelling combustion, radiation and soot processes in compartment fire. *Build Environ* 2003;38(6):771–85.
- [9] Yeoh GH, Yuen RKK, Lee EWM, Cheung SCP. Fire and smoke distribution in a two-room compartment structure. *Int J Numer Methods Heat Fluid Flow* 2002;12(2–3):178–94.
- [10] Yin R, Chow WK. Studies on thermal responses of sprinkler heads in atrium buildings with fire field model. *Fire Mater* 2001;25(1):13–19.
- [11] Okayama Y. A primitive study of a fire detection method controlled by artificial neural net. *Fire Saf J* 1991;17(6):535–53.
- [12] Ishii H, Ono T, Yamauchi Y, Ohtani S. Fire detection system by multi-layered neural network with delay circuit. *Fire safety science—proceedings of the fourth international symposium*; 1994. p. 761–72.
- [13] Milke JA, Mcavoy TJ. Analysis of signature patterns for discriminating fire detection with multiple sensors. *Fire Technol* 1995;31(2):120–36.
- [14] Pfister G. Multisensor/multicriteria fire detection: a new trend rapidly becomes state of art. *Fire Technol* 1997;33(2):115–39.
- [15] Chen Y, Sathyamoorthy S, Serio MA. New fire detection system using FT-IR spectroscopy and artificial neural network. NISTIR6242, NIST annual conference fire research, Gaithersburg, MD; 1982.
- [16] Lee WM, Yuen KK, Lo SM, Lam KC. Prediction of sprinkler actuation time using the artificial neural network. *J Build Surv* 2000;2(1):10–13.
- [17] Rosenblatt F. *Principles of neurodynamics*. New York: Spartan Books; 1962.
- [18] Carpenter GA, Grossberg S, Markuzon N, Reynolds JH. Fuzzy ARTMAP: a neural network architecture for incremental supervised learning of analog multidimensional maps. *IEEE Trans Neural Netw* 1992;3(5):698–713.
- [19] Lee EWM, Yuen RKK, Lo SM, Lam KC. Application of fuzzy ARTMAP for prediction of flashover in compartmental fire. *Proceedings of international conference on construction Hong Kong*; 19–21 June, 2001. p. 301–11.
- [20] Lee EWM, Yuen RKK, Lo SM, Lam KC. Probabilistic inference with maximum entropy for prediction of flashover in single compartment fire. *Adv Eng Inform* 2002;16:179–91.
- [21] Lee EWM, Lim CP, Yuen RKK, Lo SM. A hybrid neural network for noisy data regression. *IEEE Trans Syst Man Cybern—Part B* 2004;34(2): 951–60.

- [22] Lee EWM, Yuen RKK, Lo SM, Lam KC, Yeoh GH. A novel artificial neural network model for prediction of thermal interface location in single compartment fire. *Fire Saf J* 2004;39:67–87.
- [23] Peacock RD, Reneke PA, Bukowski RW, Babrauskas V. Defining flashover for fire hazard calculations. *Fire Saf J* 1999;32(4):331–4.
- [24] Babrauskas V, Peacock RD, Reneke PA. Defining flashover for fire hazard calculations: part II. *Fire Saf J* 2003;38(7):613–22.
- [25] Hägglund B, Jansson R, Onnermark B. Fire development in residential rooms after ignition from nuclear explosions; FOA report C 20016-D6-A3; Forsvarets Forskningsanstalt; Stockholm; 1974.
- [26] Carpenter GA, Grossberg S, David BR. Fuzzy ART: fast stable learning and categorization of analog patterns by an adaptive resonance system. *Neural Netw* 1991;4:759–71.
- [27] Specht DF. A general regression neural network. *IEEE Trans Neural Netw* 1991;2(6):568–76.
- [28] Tomandl D, Schober A. A modified general regression neural network (MGRNN) with new, efficient training algorithms as a robust ‘black box’—tool for data analysis. *Neural Netw* 2001;14:1023–34.
- [29] Lim CP, Harrison RF. Modified fuzzy ARTMAP approaches bayes optimal classification rates: an empirical demonstration. *Neural Netw* 1997;10(4):755–74.
- [30] Lim CP, Harrison RF. An incremental adaptive network for online supervised learning and probability estimation. *Neural Netw* 1997;10(5): 925–39.
- [31] Parzen E. On estimation of a probability density function and mode. *Ann Math Stat* 1962;33:1065–76.
- [32] Lang K, Whitbrock M. Learning to tell two spirals apart. Proceedings of the 1988 connectionist models summer school (June 17–26, 1988), Carnegie Mellon University. San Mateo, CA: Morgan Kaufmann Publishers Inc.; 1989. p. 52–9.
- [33] Hwang JN, You SS, Lay SR, Jou LC. What’s wrong with a cascaded correlation learning networks? A projection pursuit learning perspective, Technical report, Department of Electrical Engineering, University of Washington; 1994.
- [34] Williamson JR. Gaussian ARTMAP: a neural network for fast incremental learning of noisy multidimensional maps. *Neural Netw* 1996;9(5):881–97.
- [35] Efron B. Bootstrap methods: another look at the jackknife. *Ann Stat* 1979; 7:1–26.
- [36] Efron B. Nonparametric standard errors and confidence intervals. *Can J Stat* 1981;9:139–72.
- [37] Fisher RA. The use of multiple measurements in taxonomic problems. *Ann Eugen* 1936;7(II):179–88.
- [38] Lin CT, Lee CSG. Neural-network based fuzzy logic control and decision system. *IEEE Trans Comput* 1991;40(12):1320–36.
- [39] Quek C, Tung WL. A novel approach to the derivation of fuzzy membership functions using the Falcon-MART architecture. *Pattern Recognit Lett* 2001;22:941–58.
- [40] McCaffrey BJ, Quintiere JG, Harkleroad MF. Estimating room fire temperatures and the likelihood of flashover using fire test data correlations. *Fire Technol* 1981;17(2):98–119.
- [41] Portier RW, Peacock RD, Reneke PA. FASTLite: engineering tools for estimating fire growth and smoke transport. Special publication 899. National Institute of Standards and Technology; 1996.
- [42] Jones WW, Peacock RD. Technical reference guide for FAST version 18. National Institute of Standards and Technology; 1989.
- [43] Heskestad G. Engineering relations for fire plumes. Society of Fire Protection Engineers; Technology report; 1982. p. 82–8.